

## Polymorphism phase transition and the relative stability of various phases in the $\text{LiIO}_3$ crystal

J. K. Liang, G. H. Rao, and Y. M. Zhang

*Institute of Physics, Academia Sinica, Beijing, 100080 China*

(Received 17 February 1988; revised manuscript received 8 July 1988)

The polymorphism phase transition and relative stability of various phases in  $\text{LiIO}_3$  crystal at normal pressure have been further studied by means of  $\mu\text{DTA}$ , constant-temperature heat treatment, specific heat, and room- and high-temperature powder x-ray diffractions. There are three phases,  $\beta$ ,  $\eta$ , and  $\delta$ , existing relatively stably at high temperature, and they can directly melt at 432, 421, and 416°C, respectively. The melting points, thermal processes, and the existing temperature ranges all show that the order of their thermodynamical stability is:  $\beta > \eta > \delta$ . At room temperature the  $\alpha$ ,  $\beta$ , and  $\zeta$  can coexist in dry air. Their stabilities were determined by Gibbs free energy curves versus temperature. The  $\alpha$  phase is stable at room temperature, while the  $\beta$  phase is stable above 300°C. In the range 210–290°C, the stable phase is the  $\zeta$  phase. During heating both  $\alpha$  and  $\zeta$  phases change into the  $\beta$  phase and cannot be transformed into each other. The existence of the  $\beta$  phase in the  $\alpha$  or  $\zeta$  phase has a promotive effect on the phase transition of  $\alpha$  or  $\zeta$  into  $\beta$ . The existence of the  $\zeta$  phase in the  $\alpha$  phase also has a promotive effect on the  $\alpha$  to  $\beta$  transformation. The  $\gamma$  phase is an intermediate metastable phase in the phase transition  $\alpha \rightarrow \beta$ . The  $\theta$  phase, like the  $\gamma$  phase, is also an intermediate metastable phase through which the  $\delta$  phase changes into the  $\alpha$  phase on cooling or changes into the  $\eta$  phase on heating.

### I. INTRODUCTION

The phase transition of crystals is a very important subject rich in various phenomena and general in character and thus deserving to be studied in solid state physics. From the viewpoint of structure, it can be divided into two categories:<sup>1</sup> i.e., displacive and reconstructive phase transitions. Great progress has been achieved both in theoretical understanding and systematic experimenting with the former, including soft-mode phase transitions,<sup>2</sup> the Martensite phase transition of the  $A15$  structure,<sup>3</sup> as well as the cooperative Jahn-Teller effect induced phase transition.<sup>4</sup> As for the latter, which is quite important in practical application, e.g., the transition from graphite to diamond, however, much work has to be done in accumulating a large quantity of experimental facts so as to intensify and extend our theoretical knowledge in this connection.

The  $\alpha$  and  $\beta$  phases of  $\text{LiIO}_3$  crystals can be grown independently from the aqueous solution under different conditions and they are stable at room temperature.<sup>5–7</sup>  $\alpha\text{-LiIO}_3$  is a nonferroelectric polar crystal with its space group  $P6_3(C_6^6)$ ,<sup>8,9</sup> thus possessing excellent non-linear-optical<sup>10</sup> and piezoelectric properties.<sup>11</sup> On the contrary,  $\beta\text{-LiIO}_3$  has a symmetry center with the space group  $P4_2/n(C_{4h}^4)$ .<sup>12,13</sup> Therefore a reversion of the  $\text{IO}_3^-$  ion is needed for the transition between  $\alpha$  and  $\beta$  phases. It is expected that the solid  $\text{LiIO}_3$  may have very complex polymorphism and reconstructive phase transition problems.

Since the 1960s, it has been found by means of differential thermal analysis (DTA), high-temperature x-ray diffraction<sup>14–18</sup> that  $\alpha\text{-LiIO}_3$  can reversibly change into the  $\gamma$  phase belonging to the orthorhombic crystal system at about 250°C, which leads to a further irreversi-

ble change into the  $\beta$  phase at about 285°C, i.e.,  $\alpha \rightleftharpoons \gamma \rightarrow \beta$ . In this paper we further study the polymorphism and phase transition mechanism of solid-state  $\text{LiIO}_3$  by means of  $\mu\text{DTA}$ , specific heat, room- and high-temperature x-ray diffraction.

### II. THE PHASE TRANSITION MECHANISM AT ATMOSPHERIC PRESSURE

The phase transition mechanism has been studied by means of a home-made CR-G-type DTA ( $\mu\text{DTA}$ ) with Pt crucible. The  $\text{Al}_2\text{O}_3$  powder is used as standard and the Pt cylinder as heat equalizer. The heating and cooling temperature is at a rate of 10°C/min. All the differential temperature detection, temperature control and measurements are made with Pt-PtRh thermocouples.

The  $\alpha \xrightleftharpoons[200-190^\circ\text{C}]{240-250^\circ\text{C}} \gamma$  phase transition is reversible. The disagreement of the transition temperature during heating and cooling is due to the overheating, overcooling, and phase transition hysteresis. The phase transition  $\gamma \rightarrow \beta$  is irreversible. Its temperature of phase transition increases with the times of melting of the samples. After three cycles of melting  $\rightleftharpoons$  room temperature, the  $\gamma \rightarrow \beta$  phase transition temperature increases from 305 to 360°C.

When the highest point of endothermic peak is observed in the  $\mu\text{DTA}$  curve (430°C), the sample is lifted off the furnace or the power is switched off to produce a sudden cool. As it cools down to room temperature in this way, no other thermal effects have been observed except the exothermic peak of solidification. The sample at room temperature is identified to be  $\beta$  phase by x-ray analysis. This may probably be due to the fact that there still remains a short-order group similar to the  $\beta$  phase in

the melt near the melting point or that parts of the  $\beta$  phase have not been completely melted as nuclei.

When the sample is fully melted at 450°C and then cools down, letting it solidify, it is treated at constant temperature for more than 10 h in the  $\beta$ -phase existing temperature region. The exothermic effect can still be observed even when further cooling down to 200°C. The sample at room temperature is found to be  $\alpha$  phase by x-ray analysis. Thus, it is reasonable to infer that after the short-order of the  $\beta$ -phase lattice in the melt of  $\text{LiIO}_3$  is destroyed at heating to 450°C,  $\text{LiIO}_3$ -cools and solidifies to form a new phase  $\delta$ , which is not only different from the  $\beta$  phase of  $\text{LiIO}_3$  since the  $\beta$  phase can still remain at room temperature when cooled, but is also different from the  $\gamma$  phase because the  $\gamma$  phase should be changed into the  $\beta$  phase after annealing treatment for a long time in the  $\beta$ -phase existing temperature region. The existence of the  $\delta$  phase is proved by high-temperature x-ray diffraction with a Guinier-Lenne camera.

By melting fully and cooling to 396°C,  $\text{LiIO}_3$  solidifies exothermally to form the  $\delta$  phase. When it continues to fall to a temperature above 200°C, the room-temperature phase thus obtained through various heat treatments is determined by x-ray phase analysis and  $\mu\text{DTA}$ . The results are shown in Table I.

The  $\delta$  phase does not change at a temperature above 220°C and still holds even at a rise of temperature. By cooling to 200°C an exothermic peak can still be observed, and the  $\alpha$  phase is formed. If the  $\delta$  phase is cooled to a very narrow temperature region (200–220°C) and then increases to more than 385°C again, or it is kept

at constant temperature a bit below 385°C for a certain time (the lower the temperature, the longer the constant-temperature heat treatment will be) and then decreases to room temperature, no exothermic effect can be observed. The final resulting phase determined by the room-temperature phase analysis shows that it is neither the  $\alpha$  phase nor  $\beta$  phase, but a new phase  $\zeta$  which is metastable and coexists with the  $\alpha$  and  $\beta$  phases at room temperature. The  $\zeta$  phase releases heat and changes into the  $\beta$  phase irreversibly at a temperature of 335°C. It is supposed that the  $\zeta$  phase comes from another new high-temperature phase because none of the known phases ( $\alpha, \beta, \gamma, \delta$ ) can lead to the  $\zeta$  phase; the  $\delta$  and  $\gamma$  phases change into the  $\alpha$  phase when cooling to room temperature while the  $\alpha$  and  $\beta$  phases remain the same phase state at cooling. Meanwhile it is impossible for the  $\zeta$  phase to exist above 335°C. We therefore name this new high-temperature phase the  $\eta$  phase. The  $\eta$  phase can change into the  $\zeta$  phase only when cooling to a temperature below 160°C.

In the temperature region where the  $\delta$  and  $\eta$  phases exist, they will change into the  $\beta$  phase if fluctuation of the temperature takes place. The  $\eta$  phase does not result from the  $\delta$ -phase region on cooling. It can only be obtained when the  $\delta$  phase cools down to a temperature between 200 and 220°C and rises again at a rate of 10°C/min to a temperature above 385°C. The  $\eta$  phase cannot be obtained from known phases by heating. It is appropriate to suppose that the  $\delta$  phase changes into another intermediate phase  $\theta$  without any thermal effect on cooling down to 220°C, and by heating to 385°C the  $\theta$

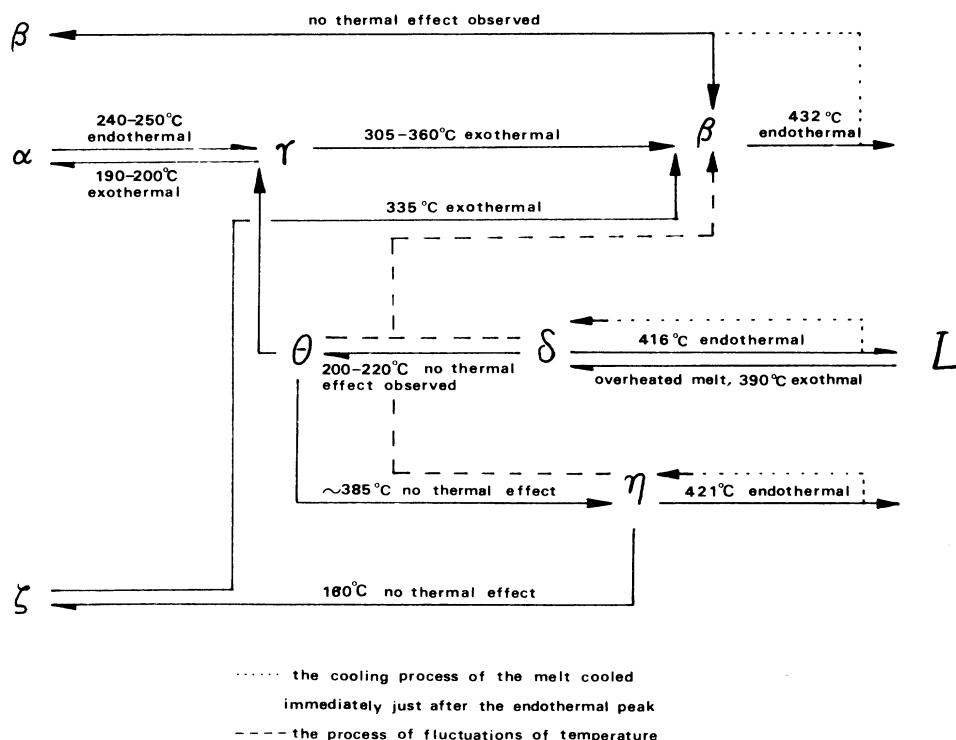


FIG. 1. The phase transition of  $\text{LiIO}_3$  crystal under atmospheric pressure.

TABLE I. The phase states through various heat treatment of the  $\delta$  phase.

Starting point of heating temperature (°C)	Heating temperature at a rate of 10°/min (°C)	Heat treatment	Thermal effect	Phase at room temperature	Note
> 220	Any temperature before melting > 385	Quenching or cooling slowly to room temperature	An exothermic peak is observed at 200°C during cooling	$\alpha$	$\delta$ phase exists above 220°C until melting point
200–220		Quenching or cooling slowly to room temperature	No thermal effect is observed	$\xi$	Heating to a temperature above 385°C, $\delta$ phase is changed into a new phase $\eta$ . By cooling, $\xi$ phase can be obtained
200–220	< 385	Quenching or cooling slowly to room temperature	An exothermic peak is observed at 200°C during cooling	$\alpha$	$\eta$ phase has not been formed while $\delta$ phase still exists, thus no $\xi$ phase can be formed
$\xi$ phase from room temperature	335 to before melting	Quenching or cooling slowly to room temperature	An exothermic peak is observed at 335°C during heating	$\beta$	$\xi$ phase is metastable at room temperature, when heating it changes exothermally into $\beta$ phase
200–220	385 to before melting	The second time cooling to below or above 160°C and then heating before melting, again quenching and cooling slowly to room temperature	Exothermic effect is observed at 335°C during the second time heating	$\beta$	$\eta$ phase during the cooling to below 160°C changes into $\xi$ phase, otherwise still remains $\eta$ phase
			No thermal effect is observed	$\xi$	

phase changes into the  $\eta$  phase without thermal effect. The formation of the  $\theta$  phase is a prerequisite for the formation of the  $\eta$  phase, while the formation of the  $\eta$  phase is a prerequisite for the formation of the  $\zeta$  phase.

To sum up, the mechanism of phase transition of  $\text{LiIO}_3$  during heating and cooling under atmospheric pressure is shown in Fig. 1.  $\text{LiIO}_3$  exhibits many phase states under atmospheric pressure, and has an extremely complex mechanism of phase transition. Furthermore, the serious heat hysteresis occurring in the phase transition of  $\text{LiIO}_3$  makes it easy for the transition process to be observed and also offers a good object in the study of reconstructive phase transition.

### III. CRYSTAL STRUCTURE OF VARIOUS PHASES IN $\text{LiIO}_3$

The sample used is an excellent single crystal of  $\alpha$ - $\text{LiIO}_3$  grown from a neutral aqueous solution. No weight loss was observed in thermogravimetry (TG) measurement below 450°C. Its aqueous solution is neutral.

The diffraction data of  $\alpha$ ,  $\beta$ , and  $\zeta$ , which can exist at room temperature, are collected by means of a RU-1000 high-power rotating-target x-ray generator (500 mA 40kV) and a SG-9R goniometer with a radius of 335 mm. The diffraction angles were calibrated by a Si standard. The lattice parameters were corrected by a least-squares method. The accuracy of diffraction angle is 0.02° with the deviation less than 0.02%. The lattice parameters of the  $\alpha$  and  $\beta$  phases are in agreement with those of Refs. 8 and 9 and Refs. 12 and 13, respectively. We further determined the diffraction angles of (00 $l$ ) and ( $h$ 00) planes of single crystal  $\alpha$ - $\text{LiIO}_3$  with a diffractometer, and the results were in agreement with those of powder diffraction measurement. The results are listed in Table II.

The  $\zeta$  phase is obtained by cooling the  $\eta$  phase to below 160°C without thermal effect. It may belong to displacive phase transition. Thus, the lattice parameters of the  $\zeta$  phase are closely related to those of the  $\eta$  phase:

$$2a(\zeta) \simeq \{a^2(\eta) + [a(\eta)/2]^2\}^{1/2},$$

i.e.,  $a(\zeta)$  is not half of the diagonal of the quadrangle plane of the  $\eta$  phase, but is that of a rectangle with  $a' = a$ ,

$b' = a/2$  in this plane; we have

$$c(\eta) \simeq \{b^2(\zeta) + [c(\zeta)/2]^2\}^{1/2},$$

i.e.,  $c(\eta)$  is decomposed into two mutual vertical vectors,  $\mathbf{b}'$  and  $\mathbf{c}'$ , and then we take  $b(\zeta) \simeq |\mathbf{b}'|$  and  $c(\zeta) \simeq 2|\mathbf{c}'|$ .

It is shown from Fig. 1 that the  $\delta$ ,  $\theta$ ,  $\gamma$ , and  $\eta$  phases cannot exist at room temperature. These phases result from special heat treatment and different phase transition paths. It is difficult to obtain their single crystals and they cannot exist at room temperature. So their diffraction data are collected by a high-temperature Guinier-Lenne monochromatic focusing camera, the  $\text{LiIO}_3$  sample is packed by Ni or Al foils with a thickness of 10  $\mu\text{m}$ , and they were also used as the inner standard. The diffraction lines of each phase are indexed by Werner's indexing program.<sup>19</sup> The lattice parameters are derived by a least-squares method. The standard deviation of the lattice parameter is 0.1% due to the broadening of high-temperature diffraction lines.

The foil is made with crisscross striations on it so that the sample might not flow out after melting. The sample is homogeneously distributed over the foil after solidification so as to ensure the quality of the high-temperature pattern. The thickness of the transmission direction of the sample is the reversal of the linear absorption coefficient of the sample. According to the phase relation indicated in Fig. 1, the high-temperature x-ray diffraction analysis of the  $\delta$ ,  $\theta$ ,  $\gamma$ , and  $\eta$  phases in  $\text{LiIO}_3$  were carried out. The high-temperature phase state can be judged by phase analysis during cooling to room temperature after respective heat treatment. The results obtained are listed in Table II and Fig. 2.

Matsumura<sup>16</sup> and Czank<sup>18</sup> reported their studies on the  $\gamma$  phase. Our result is close to that of Ref. 18, while the cell volume of the  $\gamma$  phase reported in Ref. 16 is 7.5 times greater than ours and the number of expected diffraction lines is very different from our observation. If the result of Matsumura is used to index the data of our experiment, the de Wolff merit of indexing is lower than our indexing result. It means that the reliability of the reported result<sup>16</sup> is doubtful.

There exist relations of lattice parameters between the  $\gamma$  and  $\alpha$  phases:

TABLE II. Crystal data for various phases of  $\text{LiIO}_3$  under atmospheric pressure.

Phase	Temperature	Crystal system or space group	Unit cell constants ( $\text{\AA}$ )			Unit cell formula unit	Density calculated ( $\text{g/cm}^3$ )
			$a$	$b$	$c$		
$\alpha$	Room temp.	$P6_3$	5.481(1)		5.172(1)	2	4.49
$\beta$	Room temp.	$P4_2/n$	9.733(2)		6.157(2)	8	4.14
$\zeta$	Room temp.	$P2_12_12_1$	6.498(2)	7.118(2)	12.265(3)	8	4.26
$\gamma$	230°C	Orthorhombic	9.430(10)	5.878(6)	5.321(6)	4	4.10
$\delta_1$	390°C	Cubic	6.968(7)			4	3.57
$\eta$	385°C	Tetragonal	11.563(12)		9.342(10)	16	3.87
$\theta_1$	220°C	Orthorhombic	9.505(10)	5.722(6)	10.589(10)	8	4.19
$\theta_2$	220°C	Orthorhombic	7.870(8)	7.970(8)	7.356(8)	6	3.93

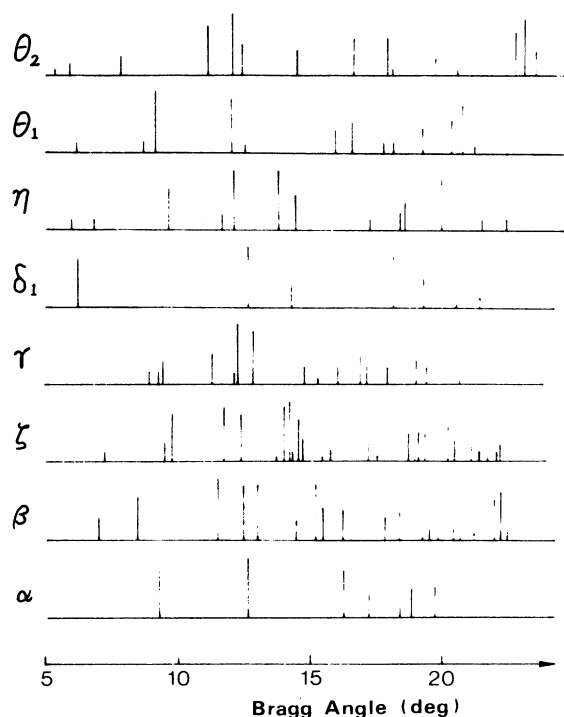


FIG. 2. X-ray diffraction powder patterns of various phases of  $\text{LiIO}_3$  crystal under atmospheric pressure,  $\text{Cu K}\alpha$  radiation.

$$a(\gamma) \simeq 2a(\alpha)\cos 30^\circ, \quad b(\gamma) \simeq a(\alpha), \quad c(\gamma) \simeq c(\alpha).$$

The relations may result from the displacement of the  $\text{IO}_3^-$  radical in the  $\alpha$  phase during heating. The displacement of  $\text{IO}_3^-$  destroy the hexagonal symmetry of the  $\alpha$  phase and forms the  $\gamma$  phase with orthorhombic symmetry.

There exists a group of  $\delta$  phases which possess different diffraction patterns owing to the fact that the solidification condition is not completely the same, or the packing material is different. Although the structure of a group of  $\delta$  phases is not the same, they all come from the

solidification through fully melting and finally change into  $\alpha$  phases on cooling to room temperature. Thus these phases all are called  $\delta$  phases. In Table II and Fig. 2 only one of a group of  $\delta$  phases is shown.

The  $\theta$  has two kinds of diffraction patterns:  $\theta_1$  and  $\theta_2$ . They all result from the  $\delta$  phase on cooling and they change to the  $\alpha$  phase when the temperature decreases, and to the  $\eta$  phase when the temperature is raised again.

The lattice parameters of the  $\theta$  phase are also closely related to those of the  $\alpha$  and  $\eta$  phases:  $a(\theta_1) \simeq 2a(\alpha)\cos 30^\circ$ ,  $b(\theta_1) \simeq a(\alpha)$ ,  $c(\theta_1) \simeq 2c(\alpha)$ , and  $c(\eta) \simeq a(\theta_1)$ ,  $a(\eta) \simeq [b^2(\theta_1) + c^2(\theta_1)]^{1/2}$ , i.e., the side of quadrangle plane of the  $\eta$  phase is the diagonal of the  $b$ - $c$  plane in the lattice cell of the  $\theta_1$  phase.

#### IV. THE PROPERTIES AND STABILITY OF VARIOUS PHASES IN $\text{LiIO}_3$

##### A. Phase states at room temperature

$\text{LiIO}_3$  has three different kinds of phase states at room temperature under atmospheric pressure:  $\alpha$ ,  $\beta$ , and  $\zeta$ . They can exist for a long time in dry air. On a DTA instrument and heating at a rate of  $10^\circ\text{C}/\text{min}$ , the  $\alpha$  phase changes into the  $\beta$  phase at  $305^\circ\text{C}$  through the  $\gamma$  phase while the  $\zeta$  phase changes into the  $\beta$  phase at  $335^\circ\text{C}$  with an exothermal effect. Once the  $\beta$  phase is formed, it cannot change into the  $\alpha$  or  $\zeta$  phase in solid state. Their relative stabilities were judged by the curves of free energy versus temperature.

The specific heat and latent heat of phase transition of  $\alpha$ -,  $\beta$ -, and  $\zeta$ - $\text{LiIO}_3$  in the range of  $-100$  to  $400^\circ\text{C}$  were measured by  $M$ - and  $L$ -type SH-3000 adiabatic scanning calorimeters made in Japan with Pt crucible. The samples were 17–20 g. The experimental condition is the same as the calibration condition. The calorimeters and Pt crucible were calibrated with standard samples  $\alpha$ - $\text{Al}_2\text{O}_3$  and  $\text{NH}_4\text{Cl}$ . The standard deviation is 3%. The experiments were carried out under purified Ar atmosphere with heating power 1.0 W, and data were taken

TABLE III. Coefficients of  $C_p$  and latent heats of various phases of  $\text{LiIO}_3$ .

Sample	Temperature ( $^\circ\text{C}$ )	$a$ ( $10^{-14}$ )	$b$ ( $10^{-11}$ )	$c$ ( $10^{-9}$ )	$d$ ( $10^{-5}$ )	$e$ ( $10^{-3}$ )	$f$ ( $10^{-1}$ )	$T_c$ ( $^\circ\text{C}$ )	$\Delta H$ (J/g)
$\alpha$	−100 to 248	−6.330	5.836	−4.012	−1.141	4.970	−1.220	248	$\alpha \rightleftharpoons \gamma$ $\pm 11.4$
	248–306 <sup>a</sup>	−6.330	5.836	−4.012	−1.141	4.970	−1.220	306	$\gamma \rightarrow \beta$ −4.84
	306–400	−1.877	0.839	1.667	0.619	−3.055	2.700		
$\zeta$	−100 to 176 <sup>b</sup>	−38.023	52.913	−277.362	6.809	−6.813	5.871		
	−100 to 310	5.647	−12.215	89.868	−2.905	5.135	0.468	310	$\zeta \rightarrow \beta$ −4.74
	310–400	−4.728	2.191	6.506	1.264	−7.954	3.215		
$\beta$	−100 to 400	0.0975	−0.118	0.254	−0.105	1.447	1.925		

<sup>a</sup>In this temperature range, high-temperature Guinier-Lenne x-ray diffraction indicated that the  $\alpha$ ,  $\beta$ , and  $\zeta$  phase could coexist. So the  $C_p$  values in this range extrapolated from that of the  $\alpha$  phase of  $-100$  to  $248^\circ\text{C}$ .

<sup>b</sup> $C_p$  values of the  $\zeta$  phase fitted with the data from  $-100$  to  $176^\circ\text{C}$ . In the range  $270$ – $310^\circ\text{C}$ , the  $C_p$  curve decreased possibly due to the exothermal effect of  $\zeta \rightarrow \beta$  transition.

every other 2 °C and fitted in terms of a 5th-order polynomial by a least squares method:

$$C_p = aT^5 + bT^4 + cT^3 + dT^2 + eT + f. \quad (1)$$

Meanwhile, we measured the latent heat of phase change of  $\text{LiIO}_3$  during heating which corresponded to the area of thermal peak in the  $C_p$  curve, and was positive for an endothermal effect, negative for an exothermal effect. Table III shows the coefficients of  $C_p$  and the latent heats for various phases of  $\text{LiIO}_3$ .

According to thermodynamic laws, the entropy  $S$ , enthalpy  $H$ , and Gibbs free-energy  $G$ , for any substance can be derived from the  $C_p$  value:

$$S^i(T) = S^i(T_0) + \int_{T_0}^T \frac{C_p}{T} dT + \sum_i \frac{\Delta H_i}{T}, \quad (2)$$

$$H^i(T) = H^i(T_0) + \int_{T_0}^T C_p dT + \sum_i \Delta H_i, \quad (3)$$

thus,

$$\begin{aligned} G^i(T) &= H^i(T) - TS^i(T) \\ &= H^i(T_0) - TS^i(T_0) + \int_{T_0}^T C_p dT - T \int_{T_0}^T \frac{C_p}{T} dT \\ &\quad + \sum_i \Delta H_i - T \sum_i \frac{\Delta H_i}{T_c}, \end{aligned} \quad (4)$$

where  $i = \alpha, \beta, \zeta$  indicate the phase state of  $\text{LiIO}_3$ .  $T$  is the absolute temperature,  $T_0$  the reference temperature,  $S^i(T_0)$  and  $H^i(T_0)$  the entropy and enthalpy at  $T_0$ , respectively.  $\Delta H^i$  is the latent heat of phase change of  $\text{LiIO}_3$  from  $T_0$  to  $T$ ,  $T_c$  is the transition temperature. When phase transitions exist,  $C_p$  values should be fitted separately according to  $T_c$ .

The experiment showed that the  $\alpha$  and  $\zeta$  phases of  $\text{LiIO}_3$  change into the  $\beta$  phase when heated to 673.15 K. In the other words, all three phases of  $\text{LiIO}_3$  have the same entropy, enthalpy, and Gibbs free-energy values when heated to 673.15 K. Let  $S(673.15\text{K}) = 0$ ,  $H(673.15\text{K}) = 0$ , then Eqs. (2)–(4) can be rewritten as

$$S^i(T) = \int_{673.15}^T \frac{C_p}{T} dT + \sum_i \frac{\Delta H_i}{T_c}, \quad (5)$$

$$H^i(T) = \int_{673.15}^T C_p dT + \sum_i \Delta H_i, \quad (6)$$

and

$$\begin{aligned} G^i(T) &= \int_{673.15}^T C_p dT - T \int_{673.15}^T \frac{C_p}{T} dT \\ &\quad + \sum_i \Delta H_i - T \sum_i \frac{\Delta H_i}{T_c}. \end{aligned} \quad (7)$$

From Eqs. (5)–(7), we can derive the entropy, enthalpy, and free-energy values of the samples at different temperatures during heating. The free-energy curves indicated the relative stabilities of  $\alpha$ -,  $\beta$ -, and  $\zeta$ - $\text{LiIO}_3$  during heating. When the temperature was above the transition point of  $\alpha \rightarrow \beta$  or that of  $\zeta \rightarrow \beta$ , the curves of the  $\alpha$ ,  $\beta$ , and  $\zeta$  phases coincided with that of the  $\beta$  phase within experi-

mental accuracy.

In order to examine the stabilities of  $\alpha$ -,  $\beta$ -, and  $\zeta$ - $\text{LiIO}_3$  under different conditions and the transition temperature at equilibrium, i.e., at which free-energies are equal, from the free-energy values including metastable parts of these three phase, we rewrote Eqs. (5)–(7) as

$$\begin{aligned} S^i(T) &= \int_{673.15}^{T_s} \frac{C_p}{T} dT + \sum_i \frac{\Delta H_i}{T_c} + \int_{T_s}^T \frac{C_p}{T} dT \\ &= S^i(T_s) + \int_{T_s}^T \frac{C_p}{T} dT, \end{aligned} \quad (8)$$

$$H^i(T) = H^i(T_s) + \int_{T_s}^T C_p dT, \quad (9)$$

and

$$\begin{aligned} G^i(T) &= [H^i(T_s) - TS^i(T_s)] \\ &\quad + \int_{T_s}^T C_p dT - T \int_{T_s}^T \frac{C_p}{T} dT, \end{aligned} \quad (10)$$

where  $T_s$  is a temperature at which phase  $i$  exists stably, e.g.,  $T_s = -100^\circ\text{C}$ . When the  $C_p$  values of phase  $i$  in its stably existing range was used extrapolatedly, Eqs. (8)–(10) give the entropy, enthalpy, and Gibbs free-energy values of phase  $i$  at extrapolated temperature  $T$  referred to as those of the  $\beta$  phase at  $400^\circ\text{C}$ . Thus, the values given by Eqs. (8)–(10) describe the Gibbs free-energy of these three phases in both stable and metastable

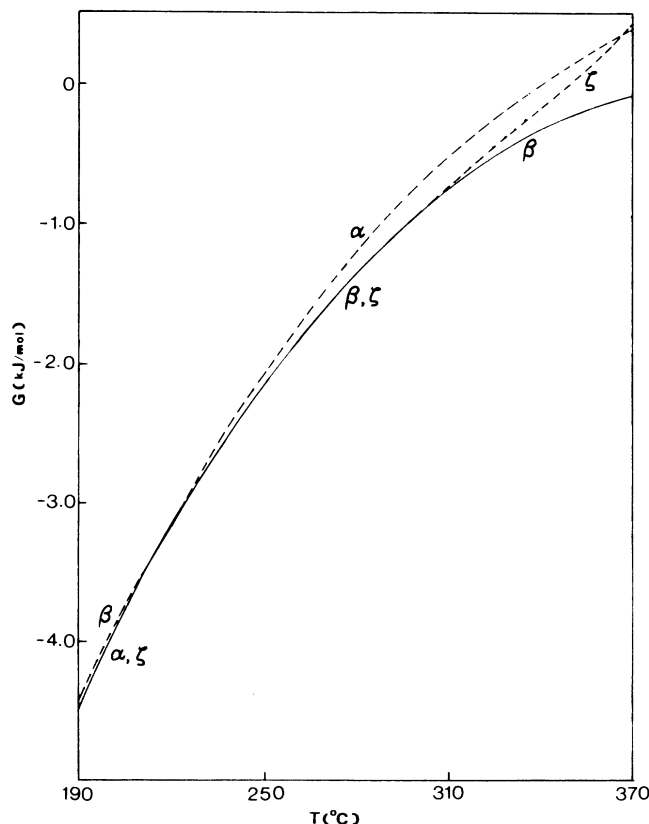


FIG. 3. Free-energy curves of  $\alpha$ ,  $\beta$ ,  $\zeta$  phases vs temperature (—, stable state; ----, metastable state).

states. We plotted the free-energy curves of the  $\alpha$ ,  $\beta$ , and  $\zeta$  phases in the range 190–370°C as shown in Fig. 3. The curve of the  $\alpha$  phase intersected that of the  $\beta$  phase at 216°C. That is to say, the equilibrium transition temperature of  $\alpha \rightleftharpoons \beta$  was 216°C. Below 216°C, the  $G$  value of the  $\alpha$  phase was smaller than that of the  $\beta$  phase, which meant that the  $\alpha$  phase was more stable, while above 216°C, the  $G$  value of the  $\alpha$  phase was greater than that of the  $\beta$  phase, which indicated that the  $\beta$  phase was more stable. The free-energy curve of the  $\zeta$  phase was nearly the same as that of the  $\alpha$  phase below 216°C and the same as that of the  $\beta$  phase in the range 216–300°C within experimental accuracy. But above 300°C the  $G$  value of the  $\zeta$  phase was obviously greater than that of the  $\beta$  phase. The results obtained by thermodynamic parameters agreed with  $\mu$ DTA and constant-temperature heat treatment.

If the  $\alpha$  phase and the  $\zeta$  phase contain the  $\beta$  phase as a crystal nucleus, the  $\beta$  nucleus will promote  $\alpha \rightarrow \beta$  and  $\zeta \rightarrow \beta$  transitions in the stable-existence temperature range of the  $\beta$  phase. That is, the  $\beta$  phase may have an induced action on both  $\alpha \rightarrow \beta$  and  $\zeta \rightarrow \beta$  transitions. This induction can only change the rate of  $\alpha \rightarrow \beta$  and  $\zeta \rightarrow \beta$  transitions, but cannot change the phase transition temperature. When constant-temperature thermal treatment is made with the  $\zeta$  phase distributed evenly in the  $\alpha$  phase, the  $\zeta$  phase does not change itself at 240°C, but promotes the rate of  $\alpha \rightarrow \beta$  phase transition. This shows that the  $\zeta$  phase also has an induced action on  $\alpha \rightarrow \beta$  phase transition.

#### B. Phase states at high temperature

$\text{LiIO}_3$  has three different kinds of phase states in the high-temperature range— $\beta$ ,  $\eta$ , and  $\delta$ . The  $\beta$ ,  $\eta$ , and  $\delta$  phases obtained by different thermal treatments do not change into each other below the melting point and directly melt themselves. On cooling to room temperature,  $\beta$  remains unchanged, while  $\delta$  and  $\eta$  change into the  $\alpha$  and  $\zeta$  phases, respectively. In order to verify the phase state of  $\text{LiIO}_3$  before melting point, the room-temperature phase analysis of the sample obtained is carried out after the top of the melting endothermic peak of each phase in the DTA curve appears, and then the furnace is lifted to make temperature cool down abruptly to room temperature. In this case of incomplete melting each phase retains the short-order group in melt or still reserves a small quantity of the original phase. As crystal nuclei they induced melting to form corresponding original phases on cooling. The melting point of various phases was determined by extrapolated onset of thermal peak of the  $\mu$ DTA curve. In order to avoid the effects on the measurement of melting temperatures due to the different contacts of the crucible and samples as well as the different sequence of melting-point measurement of each phase, three groups of experiments have been made. In the first group the formation of three phases and their melting sequence are  $\beta$ ,  $\eta$ , and  $\delta$ . In the second group the sequence of measurement is  $\eta$ ,  $\delta$ ,  $\beta$ , whereas in the third group it is  $\delta$ ,  $\beta$ ,  $\eta$ . The experimental results of the three groups are all the same. The melting point by

$\mu$ DTA measurement is corrected with crystal quartz ( $\text{SiO}_2$ ) phase transition at 573°C. All experiments were carried out under the same conditions. The measurement accuracy is better than  $\pm 1^\circ\text{C}$ . The melting points of  $\beta$ ,  $\eta$ , and  $\delta$  are 432, 421, and 416°C, respectively. This fact indicates that the initial energy required to destroy the periodic arrangement of the  $\beta$ ,  $\eta$ , and  $\delta$  lattice into a disordered liquid is different. The order is  $\beta > \eta > \delta$ . The temperature range in which the  $\beta$  phase can exist extends right to room temperature. The  $\eta$  phase can exist at a temperature above 160°C while the  $\delta$  phase can only exist above 220°C. The  $\delta$  phase can change into the  $\eta$  phase through special heat treatment. The  $\delta$  and  $\eta$  phases change into the  $\beta$  phase through temperature fluctuation. Thus, it can be considered that the order of their thermal stability is  $\beta > \eta > \delta$  from their melting points, the thermal processing, as well as their existing temperature range.

#### C. The intermediate phases $\gamma$ and $\theta$

The  $\gamma$  phase is the intermediate metastable transitional phase of phase transition  $\alpha \rightarrow \beta$ . The constant-temperature heat treatment and  $\mu$ DTA results indicate that the lowest transition temperatures of  $\alpha \rightarrow \gamma$  and  $\gamma \rightarrow \beta$  are the same, being about 240°C. The  $\gamma$  phase does not have a stable-existence temperature range. It is only a transitional phase existing in a certain temperature range (240–300°C) and at a certain time (the higher the temperature, the shorter its existing time). At the same time this temperature range is also the nucleation-growth period for  $\gamma \rightarrow \beta$ . In the temperature of  $\alpha \rightarrow \gamma$  phase transition, the  $\alpha$  phase changes gradually into the  $\gamma$  phase. If the time of heat treatment is shorter than the nucleation-growth period for the  $\beta$  phase at this temperature followed by cooling immediately, the  $\beta$  phase will not appear. For example, when the  $\alpha$ - $\text{LiIO}_3$  single crystal is kept at 240°C for constant-temperature heat treatment for 24 h, it is found that although it becomes a milky opaque split piece after cooling, it remains the  $\alpha$  phase on x-ray analysis. That is to say, at 240°C and 24 h, which is shorter than the nucleation-growth period of the  $\beta$  phase, no  $\beta$  phase can be observed. The crystal experiences reversible  $\alpha \rightleftharpoons \gamma$  phase transition and becomes cracked. With increasing temperature, the nucleation-growth period of the  $\beta$  phase becomes shorter and shorter. On heating above 300°C, the  $\gamma \rightarrow \beta$  transition rate becomes faster and thermal peaks appear on the  $\mu$ DTA curve. The  $\text{LiIO}_3$  solid solution containing  $\text{HIO}_3$  can shorten the nucleation-growth period of the  $\beta$  phase, and the exothermal effect of  $\gamma \rightarrow \beta$  phase transition cannot be observed.

Similarly to the case in the  $\gamma$  phase, the  $\theta$  phase is also an intermediate metastable transitional phase through which the  $\delta$  phase changes into the  $\alpha$  phase on cooling or changes into the  $\eta$  phase on reheating. After the  $\theta$  phase is formed, its existing temperature range is 200–385°C at at heating rate of 10°C/min, a bit wider than the existing temperature range of the  $\gamma$  phase. The  $\theta$  phase is the same as the  $\gamma$  phase, the lower the temperature, the longer its existence. At 365°C, the  $\theta$  phase exists for 2 h while at 350°C, it can exist for 8 h. That means it has the

same feature as the intermediate metastable transitional phase.

## V. FEATURES OF PHASE TRANSITION IN $\text{LiIO}_3$

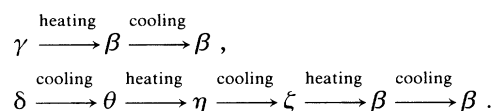
### A. The sluggish phenomena of phase transition

By using a Guinier-Lenne high-temperature monochromatic focusing camera and high-power rotating x-ray generator RU-1000, with the corresponding changes of photograph positions with temperature, we can observe the continuous change of phase state with temperature. When  $\alpha\text{-LiIO}_3$  is heated to 245–250°C, the  $\gamma$  phase begins to appear. But at this time there still remain a great number of diffraction lines belonging to the  $\alpha$  phase. The intensity of the  $\gamma$  phase increases as the temperature increases. When it reaches 270–280°C, it completely changes into the  $\gamma$  phase. When the  $\gamma$  phase is cooled, the  $\alpha$  phase begins to appear at 200–190°C, including also a large amount of the  $\gamma$ . With the temperature decreasing continuously, the  $\gamma$  phase disappears gradually. It is only down to a temperature of 110°C that it can completely change into the  $\alpha$  phase. The end of the phase transition temperature is not fixed. It depends on the rate of heating and cooling. The  $\gamma$  phase changes into the  $\beta$  phase irreversibly at 300°C. Similarly, there is still a superheating temperature range of 20°C in the  $\gamma$  phase. That is, in the phase transition there is a very wide temperature range and a long time of coexistence of two phases. The temperature of thermal effect shown in the  $\mu\text{DTA}$  curve is the temperature at which the new phase begins to appear. The same obvious sluggish phenomena also exist in  $\zeta \rightarrow \beta$  and  $\theta \rightarrow \eta$ , etc., phase transitions. At equilibrium state, the phase transition temperature for  $\zeta \rightarrow \beta$  is about 295°C, whereas that appearing in the  $\mu\text{DTA}$  curve at a heating rate of 10°C/min is 335°C, and its superheating temperature reaches 40°C. The  $\theta \rightarrow \eta$  phase transition at the equilibrium state is below 350°C, but higher than 385°C at a heating rate of 10°C/min. Its superheating temperature also exceeds

35°C. The sluggish phenomena in  $\text{LiIO}_3$  phase transition is the one often occurring in reconstructive phase transition. This is due to the fact that only when the crystal nucleus reaches the critical size needed by the fluctuation due to thermal agitations can it surmount the potential barrier and form the new phase.

### B. The irreversibility of phase transition

For instance, we have



That is probably because the phase transition on  $\text{LiIO}_3$  changes the orientation of the  $\text{IO}_3^-$  radical in the lattice, and it is not easy to restore the orientation. The  $\beta$  phase has a symmetry center and the orientation of the  $\text{IO}_3^-$  radical has a reverse arrangement thus leading to a very stable crystal structure. Therefore, if the change of the  $\beta$  phase into other phases is required, the rearrangement of the  $\text{IO}_3^-$  radical in solidification after melting is needed to change through the  $\delta$  phase into other various phases.

### C. Different structure in the same temperature range

Phases of different structure can be formed in the same temperature range. It is difficult for them to change into each other. Even under almost the same conditions,  $\text{LiIO}_3$  melt can form a group of  $\delta$  phases with different structures on cooling and solidification. No transformation of each other has also been observed in constant temperature photographs taken at high temperature for a long time. The x-ray diffraction pattern is mainly attributed to the position of  $\text{IO}_3^-$  radicals in the lattice. It is reasonable to hold that the difference of free-energy of various distribution states of  $\text{IO}_3^-$  radicals in the lattice is very small on solidification. This leads to the versatility of  $\text{LiIO}_3$  phase structure and complication of phase transition mechanism.

<sup>1</sup>M. J. Buerger, in *Phase Transformations in Solids*, edited by R. Smoluchowski *et al.* (Wiley, New York, 1951), pp. 163–211.

<sup>2</sup>*Structural Phase Transitions and Soft Modes*, edited by E. J. Samuelsen *et al.* (Universitetsforlaget, Oslo, 1971).

<sup>3</sup>M. Weger *et al.*, *Solid State Phys.* **28**, 2 (1973).

<sup>4</sup>M. D. Sturge, *Solid State Phys.* **20**, 92 (1967).

<sup>5</sup>L. Liebertz, *Z. Phys. Chem.* **67**, 94 (1969).

<sup>6</sup>D. S. Robertson and J. M. Roslington, *J. Phys. D* **4**, 1582 (1971).

<sup>7</sup>J. M. Desvignes and M. Remoissenet, *Mater. Res. Bull.* **6**, 705 (1971).

<sup>8</sup>A. Rosenzweig *et al.*, *Acta Crystallogr.* **20**, 758 (1966).

<sup>9</sup>A. Emiralieb *et al.*, *Kristallografiya* **18**, 1177 (1973).

<sup>10</sup>F. R. Nash *et al.*, *J. Appl. Phys.* **40**, 5201 (1969).

<sup>11</sup>A. W. Warner *et al.*, *J. Acoust. Soc. Am.* **47**, 791 (1970).

<sup>12</sup>L. A. Azaroba *et al.*, *Dok. Akad. Nauk SSSR* **206**, 613 (1972).

<sup>13</sup>H. Schultz, *Acta Crystallogr., Sect. B* **29**, 2285 (1973).

<sup>14</sup>F. Herlach, *Helv. Phys. Acta* **34**, 305 (1961).

<sup>15</sup>T. Umezawa *et al.*, *J. Appl. Crystallogr.* **3**, 417 (1970).

<sup>16</sup>S. Matsumura, *Mater. Res. Bull.* **6**, 469 (1971).

<sup>17</sup>H. Arend *et al.*, *Mater. Res. Bull.* **7**, 869 (1972).

<sup>18</sup>M. Czank *et al.*, *Z. Kristallogr.* **143**, 99 (1976).

<sup>19</sup>R. E. Werner, *J. Appl. Crystallogr.* **9**, 216 (1976).